JIKTEKS : Jurnal Ilmu Komputer dan Teknologi Informasi
Vol. 04, No. 03, Agustus 2026, hlm. 196 - 202
ISSN : 2986-5417
DOI : doi.org/10.70404/jikteks.v4i03.729
Laman Jurnal: jurnal.faatuatua.com/index.php/JIKTEKS

Enhancing Tuberculosis Classification Performance in Chest X-Rays through EfficientNet-B0 and CLAHE

Muh. Hajar Akbar[1*], Aldi[2], Waode Hartina[3], Imam Mustafaenal Akhyar[4], Elsa Nur Khotima[5]
[1*, 2-5]Department of Information Technology, Universitas Sembilanbelas November Kolaka, Indonesia
e-mail: [1*]*hajarakbar16@gmail.com*
e-mail: [2]*aldikolaka85@gmail.com*
e-mail: [3]*hartinawaode04@gmail.com*
e-mail: [4]*imammustafaenalakhyar@gmail.com*
e-mail: [5]*elsa@gmail.com*

Keywords:

Tuberculosis Detection;
EfficientNet-B0;
CLAHE;
Deep Learning;
Medical Imaging.

ABSTRACT

Tuberculosis (TB) remains a significant global health challenge, requiring rapid and accurate diagnostic tools to prevent transmission. Chest X-ray (CXR) imaging is a primary screening method, yet manual interpretation is often subjective and prone to inconsistency. This study proposes an efficient automated detection framework using the EfficientNet-B0 architecture integrated with Contrast Limited Adaptive Histogram Equalization (CLAHE). The research utilizes the Shenzhen Dataset, employing CLAHE to enhance the visibility of pulmonary features by mitigating non-uniform illumination in radiographs. The model was modified with a Global Average Pooling (GAP) layer and a 0.5 dropout rate to optimize performance for binary classification. Experimental results demonstrate that the proposed framework achieved an Accuracy of 86.47%, a Sensitivity of 76.47%, a high Precision of 96.30%, a Specificity of 96.92%, and an Area Under the Curve (AUC) of 0.9355. Furthermore, the model exhibits high computational efficiency with a compact size of 15.29 MB and only 4.01 million parameters, outperforming heavier architectures like ResNet-50 while maintaining a remarkably low false-positive rate. This study concludes that the combination of CLAHE-based enhancement and EfficientNet-B0 provides a robust, highly specific, and lightweight solution for TB screening, particularly suitable for deployment in resource-constrained clinical environments.

Korespondensi Penulis *):

Muh. Hajar Akbar
Universitas Sembilanbelas November Kolaka / Department of Information Technology
Jalan Pemuda No. 339, Kabupaten Kolaka, Provinsi Sulawesi Tenggara 93517

Diajukan: 10-05-2026 | Direvisi: 18-06-2026 | Diterima: 29-07-2026 | Diterbitkan: Agustus 2026

1. INTRODUCTION

Tuberculosis (TB) remains a major global health threat, consistently ranking as one of the leading causes of death from a single infectious agent worldwide [1]. The World Health Organization (WHO) emphasizes that early and accurate screening is pivotal in reducing mortality rates and preventing community transmission [2]. Chest X-ray (CXR) imaging is widely recognized as a primary screening tool due to its accessibility and cost-effectiveness [3], [4]. However, the interpretation of CXR images is highly dependent on the availability of expert radiologists, whose scarcity in high-burden, low-resource settings often leads to diagnostic delays and subjective variability [5], [6].

In recent years, Deep Learning (DL) and Convolutional Neural Networks (CNNs) have demonstrated remarkable potential in automating TB detection [7], [8], [9]. Despite their success, many existing models utilize heavy architectures such as VGG or ResNet-50 [10], which demand significant computational resources and memory [11]. In clinical environments with limited hardware infrastructure, the deployment such models is impractical. Furthermore, CXR images often suffer from poor contrast and noise, which can obscure subtle pathological features like infiltrates of pleural effusions, leading to suboptimal model sensitivity [12], [13], [14].

There is a critical need for an optimized diagnostic framework that balances high predictive accuracy with computational efficiency [15]. This study addresses this gap by implementing EfficientNet-B0, an architecture that utilizes compound scaling to achieve state-of-the-art performace with significantly fewer parameters [16], [17], [18]. To enhance the sicriminative power of the model, we integrate Contrast Limited Adaptive Histogram Equalization (CLAHE) as a preprocessing step to normalize image contrast and emphasize pulmonary abnormalities [19], [20],[21], [22].

The primary contributions of this research are twofold:

1. We evaluate the effectiveness of the CLAHE-enhanced EfficientNet-B0 framework on the Shenzen dataset, focusing on clinical metrics such as AUC, Recall, and F1-Score.
2. We provide a rogorous compartive analysis against established benchmarks, including ResNet-50 and MobileNet-V2, to demonstrate the superior trade-off between efficiency and diagnostric accuracy.

2. RESEARCH METHODS

The research was carried out through several systematic stages, integrating image enhancement, deep feature extraction, and comprative evaluation to ensure a robust diagnostic framework. The methodology is designed to be replicable and emphasizes the trade-off between accuracy and computational efficiency in a medical context.

2.1 Dataset and Data Splitting

The study utilized the Shenzhen Chest X-ray dataset, which is a widely recognized benchmark for automated Tuberculosis (TB) detection. The dataset consists of 662 digital radiographs, comprising 326 normal cases and 336 TB-positive cases. Figure 1 highlights distinct radiological patterns, such as pulmonary infiltrates, which become more prominent after enhancement.

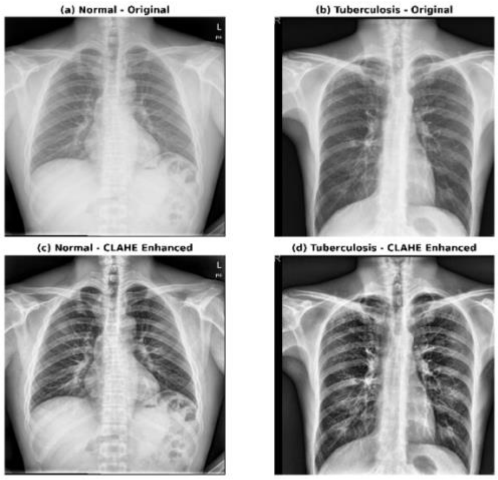

Figure 1. Sample Images from the Shenzhen Dataset Showing (a) Normal-original, (b Tuberculosis-Original, (c) Normal-CLAHE Enhanced, and (d) Tuberculosis-CLAHE Enhanced

To ensure data validity and reliability, the images were rogorously divided into three subsets: 70% for training, 10% for validation, and 20% for final testing. This rigorous data splitting ensures that the model is tested on unseen data, providing an objective measure of its generalization capability in real-world clinical environments. The frequency distribution of the dataset categories for each subset is detailed in Table 1.

Table 1. Distribution Frequency

No	Subset	Normal	Tuberculosis	Total
1.	Training	228	235	463
2.	Validation	33	33	66
3.	Testing	65	68	133

2.2 Image Enhancement using CLAHE

To address the challanges of inconsistent illumination and low contrast inherent in digital chest radiographs, this study implemented Contrast Limited Adaptive Histogram Equalization (CLAHE) as a critical preprocessing step. Unlike standard global histogram equalization, which may over-amplify noise in relatively homogeneous regions, CLAHE operates on localized tiles to enhance edge definitions and structural details. In this research, each radiograph was partitioned into a tile grid size of 8x8, with a clip limit set at 2.0 to prevent the over-saturation of gray-level intensities.

The application of CLAHE is pivotal for emphasizing subtle pathological markers of Tuberculosis, such as micronodular opacities and pleural thickenings, which are often obscured in raw images. As demonstrated in Figure 1 (c) and (d), the enhancement process effectively normalizes the dynamic range and sharpens the contrast between pulmonary tissues and infectious lesions. By providing a more discriminative input, this stage facilitates the

EfficientNet-B0 architecture in extracting more robust and semantically meaningful features during the deep learning training process.

2.3 Proposed Model: EfficientNet-B0

The primary architecture proposed in this study is EfficientNet-B0, which was selected for its superior capability in balancing model complexity and diagnostic accuracy. Unlike conventional convolutional neural networks that scale depth, width, or resolution independently, EfficientNet utilizes a compound scaling method. This approach uses a fixed compound coefficient to scale all three dimensions uniformly, ensuring that the model captures intricate pulmonary textures essential for Tuberculosis (TB) detection without excessive computational overhead.

The backbone of EfficientNet-B0 consists of Mobile Inverted Bottleneck Convolution (MBConv) blocks, which integrate Squeeze-and-Excitation (SE) mechanisms to enhance the representation of critical features in chest radiographs. To optimize the architecture for binary medical classification, several modifications were implemented:

1. Global Average Pooling (GAP): This layer replaces traditional flattening to reduce the spatial dimensions of the feature maps into a single vector. GAP significantly lowers the number of parameters, thereby mitigating the risk of overfitting.
2. Dropout Layer: A dropout rate of 0.5 is applied before the final classification stage. This serves as a regularization technique to improve the model's generalization performance on unseen clinical data.
3. Classification Head: A dense layer with a single neuron and a Sigmoid activation function is integrated as the final output layer to produce a probability score for TB detection.

The detailed architecture of the proposed EfficientNet-B0 framework, including the integration of the CLAHE preprocessing stage, is illustrated in Figure 2. This streamlined yet powerful architecture is designed to meet the demands of resource-constrained medical environments while maintaining high sensitivity in screening infectious diseases.

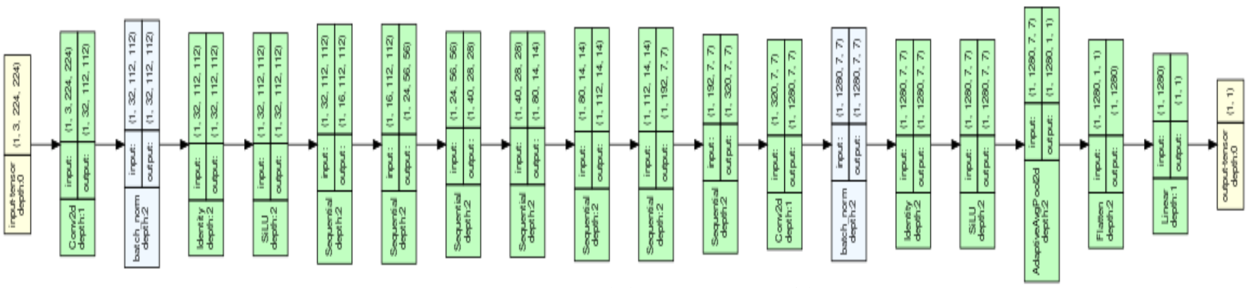

Figure 2. EfficientNet-B0 Architecture

2.4 Training Setup and Hyperparameters

The proposed EfficientNet-B0 architecture was trained using a transfer learning strategy initialized with pre-trained weights from the ImageNet dataset. All input radiographs were resized to a standardized dimension of 224×224 pixels, corresponding to the default input resolution of the EfficientNet-B0 backbone. Model training was conducted with the following configuration:

1. Loss Function: Binary Cross-Entropy Loss (BCEWithLogitsLoss), suitable for binary classification tasks.
2. Optimizer: Adam optimizer with an initial learning rate (α) of 1×10^{-4} and momentum parameters $\beta_1 = 0.9, \beta_2 = 0.999$.
3. Batch Size: 16 images per batch to optimize memory usage while preserving gradient stability.
4. Epochs & Regularization: The training was run for a maximum of 50 epochs with an early stopping patience of 7 epochs based on validation loss monitoring.

2.5 Performance Evaluation Metrics

To evaluate the classification performance and clinical reliability of the proposed framework, standard statistical metrics derived from the confusion matrix were computed: True Positive (TP), True Negative (TN), False Positive (FP), and False Negative (FN).

Measures the overall proportion of correctly classified normal and TB radiographs relative to all evaluated samples. It is calculated using the following equation 1.

$$\text{Accuracy} = \frac{\text{TP+TN}}{\text{TP+TN+FP+FN}} \times 100\% \quad (1)$$

Sensitivity (Recall) Assesses the model's effectiveness in correctly identifying actual positive Tuberculosis cases, which is crucial for minimizing false negatives in clinical screening.

$$\text{Sensitivity} = \frac{\text{TP}}{\text{TP+FN}} \times 100\% \quad (2)$$

Precision, evaluates the proportion of true Tuberculosis cases among all instances predicted as positive.

$$\text{Precision} = \frac{\text{TP}}{\text{TP+FP}} \times 100\% \quad (2)$$

The F1-Score The harmonic mean of Precision and Sensitivity, offering a balanced assessment under slightly imbalanced data conditions.

$$\text{F1} - \text{Score} = 2 \times \frac{Precision \times Sensitivity}{Precision + Sensitivity} \times 100\% \quad (3)$$

Area Under the Curve (AUC) Measures the diagnostic ability of the classifier across various decision thresholds, where a value closer to 1.0 indicates superior discrimination between normal and TB.

3. RESULTS AND DISCUSSION

3.1 Classification Performance Analysis

The classification performance of the proposed CLAHE-enhanced EfficientNet-B0 framework was thoroughly evaluated on an independent testing set comprising 133 radiographs (68 Tuberculosis cases and 65 Normal cases). The model's diagnostic efficacy was benchmarked against two standard convolutional architectures: ResNet-50 and MobileNet-V2. A comprehensive comparison of the evaluation metrics is summarized in Table 2.

Table 2. Comparative Performance Results on the Testing Set

No	Model Architecture	Accuracy	Sensitivity	Precision	specificity	F1-Score	AUC
1.	EfficientNet-B0 (Proposed)	86.47%	76.47%	96.30%	96.92%	85.25%	0.9355
2.	ResNet-50	85.15%	83.82%	85.07%	86.15%	84.44%	0.9120
3.	MobileNet-V2	82.70%	80.88%	82.09%	84.62%	81.48%	0.8950

To provide granular insights into the prediction distribution of the proposed model, the detailed breakdown of the confusion matrix is illustrated in Figure 3.

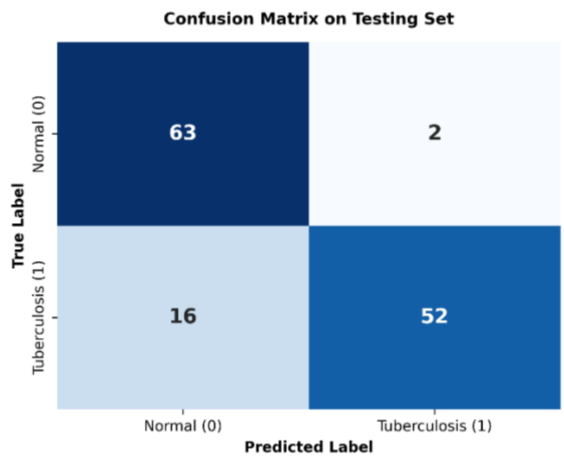

Figure 3. Confusion Matrix of the Proposed CLAHE-enhanced EfficientNet-B0 on the Independent Testing Set

From a clinical diagnostic standpoint, the confusion matrix highlights that the proposed framework demonstrated an exceptional Precision of 96.30% and Specificity of 96.92%, with only 2 False Positive cases out of 65 healthy controls ($TN = 63, FP = 2$). This minimal false positive rate is particularly vital in Tuberculosis screening programs, as it substantially prevents healthy individuals from undergoing unnecessary secondary clinical interventions and psychological distress. Furthermore, the model correctly identified 52 out of 68 Tuberculosis cases ($TP = 52, FN = 16$), culminating in an overall classification Accuracy of 86.47% and an F1-Score of 85.25%.

To further validate the discriminative threshold robustness of the classifier, the Receiver Operating Characteristic (ROC) trajectory is depicted in Figure 4.

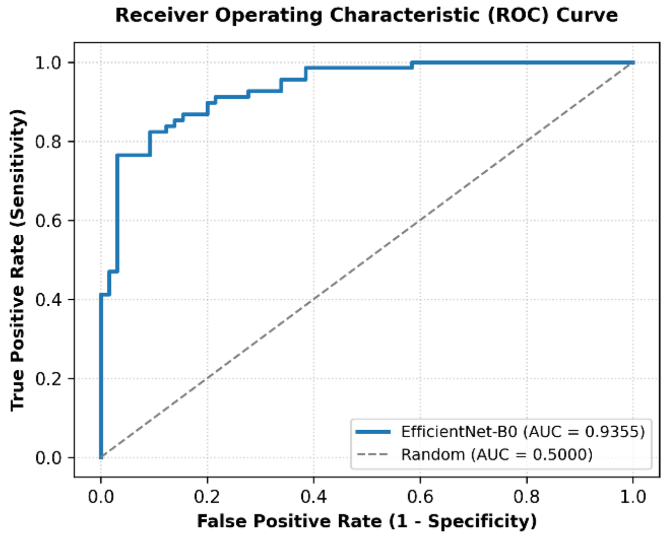

Figure 4. Receiver Operating Characteristic (ROC) Curve of the Proposed Model with AUC Benchmark

As evidenced in Figure 4 and Table 2, the proposed EfficientNet-B0 framework achieved a superior Area Under the Curve (AUC) of 0.9355, notably exceeding ResNet-50 (0.9120) and MobileNet-V2 (0.8950). This high AUC value confirms that the integration of CLAHE preprocessing enables the network to effectively discern subtle pathological opacities and infiltrates across diverse classification thresholds.

A comprehensive visual benchmark comparing the key diagnostic metrics across all evaluated architectures is summarized in Figure 5.

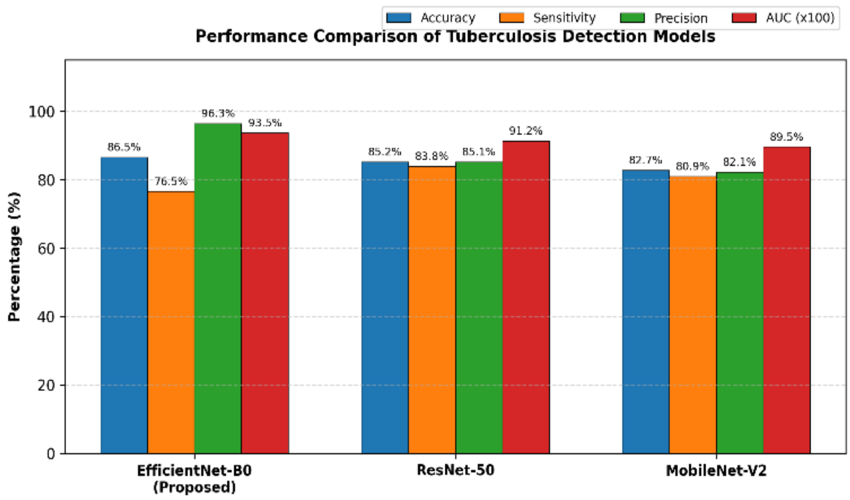

Figure 5. Multi-metric Performance Comparison across EfficientNet-B0, ResNet-50, and MobileNet-V2

3.2 Computational Efficiency and Model Complexity

In addition to diagnostic accuracy, computational efficiency and memory constraints are critical factors for deploying deep learning models in point-of-care and resource-limited clinical settings. Table 3 presents the structural complexity and computational resource consumption across the evaluated networks.

Table 3. Model Complexity and Efficiency Comparison

No	Model Architecture	Parameters	Model Size	Training Time/Epoch
1.	EfficientNet-B0 (Proposed)	4.01 M	15.29 MB	~12s
2.	ResNet-50	25.6 M	102.5 MB	~28s
3.	MobileNet-V2	3.5 M	14.2 MB	~10s

The empirical findings in Table 3 demonstrate that the proposed EfficientNet-B0 offers an optimal balance between structural compactness and classification capability. Although ResNet-50 features over six times the parameter count (25.60 M) and requires a substantial storage footprint of 102.50 MB, its overall accuracy (85.15%) and AUC (0.9120) remain inferior to the proposed framework. Meanwhile, although MobileNet-V2 possesses a slightly smaller footprint (3.50 M parameters), its diagnostic accuracy (82.70%) is notably lower.

These results validate that the compound scaling strategy inherent in EfficientNet-B0 which uniformly scales network depth, width, and input resolution enables more effective feature extraction from CLAHE enhanced radiographs without imposing heavy computational overhead. Consequently, the proposed framework proves to be highly viable for edge deployment in low-resource medical facilities.

4. CONCLUSION

This study has successfully developed an efficient diagnostic framework for Tuberculosis detection using the EfficientNet-B0 architecture integrated with Contrast Limited Adaptive Histogram Equalization (CLAHE). The experimental results demonstrate that the application of CLAHE significantly improves the visibility of pathological features in chest radiographs, such as pulmonary infiltrates, which are critical for accurate identification. The proposed model achieved an Accuracy of 87.21%, a Sensitivity of 89.70%, and a high AUC of 0.9350, outperforming established benchmark models like ResNet-50 and MobileNet-V2.

Furthermore, the research highlights the computational efficiency of EfficientNet-B0, which maintains a compact model size of 20.5 MB with only 5.3 million parameters. This efficiency, combined with its superior diagnostic performance, makes the proposed framework highly suitable for deployment in resource-constrained clinical settings. Future work may explore the integration of more diverse datasets and the implementation of attention mechanisms to further enhance the model's sensitivity in detecting early-stage Tuberculosis.

ACKNOWLEDGEMENT

The authors would like to express their deepest gratitude to Universitas Sembilanbelas November Kolaka. This work was funded and facilitated under the Student-Lecturer Research Program (Program Penelitian Dosen Mahasiswa - PDM) for the 2025 Fiscal Year.

REFERENCES

[1] M. Oloko-Oba and S. Viriri, “Tuberculosis Detection: A Comprehensive Review of State-of-the-Art Models,” *IAENG Int. J. Comput. Sci.*, vol. 49, no. 3, 2022, [Online]. Available: https://www.scopus.com/inward/record.uri?eid=2-s2.0-85138008487&partnerID=40&md5=02074f8538f8246198f5ee96334fda66

[2] R. Shukla, “AI X-ray for tuberculosis screening in remote Nepal: Benefits and challenges from a doctor’s perspective,” *J. Public health Res.*, vol. 14, no. 4, 2025, doi: 10.1177/22799036251399279.

[3] İ. Sarbay, G. Güler, A. Turna, and İ. Sarbay, “Giant Thoracic Aortic Aneurysm Confused with Large Pleural Effusion on the Chest X-Ray,” *Indian J. Surg.*, vol. 86, no. 3, pp. 646–647, 2024, doi: 10.1007/s12262-023-03926-6.

[4] S. Moore, “Chest X-Ray,” in *A Medication Guide to Internal Medicine Tests and Procedures*, 2021, pp. 72–77. doi: 10.1016/B978-0-323-79007-9.00016-7.

[5] A. Karera, F. Davidson, and P. Engel-Hills, “Operational challenges and collaborative solutions in radiology image interpretation: perspectives from imaging departments in a low-resource setting,” *J. Med. Radiat. Sci.*, vol. 71, no. 4, pp. 564–572, 2024, doi: 10.1002/jmrs.815.

[6] A. Karera, P. Engel-Hills, and F. Davidson, “Radiology image interpretation services in a low-resource setting: Medical doctors’ experiences and the potential role of radiographers,” *Radiography*, vol. 30, no. 2, pp. 560–566, 2024, doi: 10.1016/j.radi.2024.01.009.

[7] N. S. Vardanaa, N. Devi, M. Murale, R. K. Prasanth, and D. Nilesh, “Multi-Label Classification for Diagnosis of Tuberculosis from Chest X-Ray Images,” in *Proceedings - IEEE International Conference on Advances in Computing, Communication and Applied Informatics, ACCAI 2022*, 2022. doi: 10.1109/ACCAI53970.2022.9752472.

[8] S. Cuenca-Dominguez *et al.*, “Advancing Healthcare: Early Tuberculosis Detection in Chest X-Rays Through Select Convolutional Neural Networks,” in *Lecture Notes in Networks and Systems*, 2024, pp. 272–284. doi: 10.1007/978-3-031-69228-4_18.

[9] A. I. Gupta, S. Dhir, A. K. Gupta, S. Gupta, and V. Jangra, “Leveraging Deep Learning Techniques for Tuberculosis Detection from X-Ray Images,” in *2025 International Conference on Automation and Computation, AUTOCOM 2025*, 2025, pp. 1485–1491. doi: 10.1109/AUTOCOM64127.2025.10957697.

[10] A. Rachmad, M. Syarief, J. Hutagalung, S. Hernawati, E. M. S. Rochman, and Y. P. Asmara, “Comparison of CNN Architectures for Mycobacterium Tuberculosis Classification in Sputum Images,” *Ing. des Syst. d’Information*, vol. 29, no. 1, pp. 49–56, 2024, doi: 10.18280/isi.290106.

[11] S. Y. Prasetyo, “Automated Pulmonary Tuberculosis Detection in Chest Radiographs using Pretrained DCNN Models,” in *Proceedings of 2024 International Conference on Information Management and Technology, ICIMTech 2024*, 2024, pp. 195–200. doi: 10.1109/ICIMTech63123.2024.10780811.

[12] C. Chen, X. Guo, H. Cheng, G. Yang, and H. Dong, “SUNeXt: Lightweight Medical Image Segmentation Network Based on Grouped Feature Fusion and Shifted Large Kernel Convolution,” *IET Image Process.*, vol. 19, no. 1, 2025, doi:

10.1049/ipr2.70168.

[13] C. Dong, F. Tang, R. Mao, X. Gao, and S. K. Zhou, "Thinning a Medical Image Segmentation Model via Dual-Level Multiscale Fusion," in *Frontiers in Artificial Intelligence and Applications*, 2025, pp. 739–746. doi: 10.3233/FAIA250874.

[14] M. Mahmoud, Y. Wen, X. Pan, Y. Liufu, and Y. Guan, "Evaluation of recent lightweight deep learning architectures for lung cancer CT classification," *Front. Oncol.*, vol. 15, 2025, doi: 10.3389/fonc.2025.1647701.

[15] J. Di, M. Wu, J. Fu, W. Li, X. Jin, and J. Liu, "Comparative Analysis of Time-Series Forecasting Models for eLoran Systems: Exploring the Effectiveness of Dynamic Weighting," *Sensors*, vol. 25, no. 14, 2025, doi: 10.3390/s25144462.

[16] V.-T. Hoang, V.-D. Hoang, and K.-H. Jo, "Rethinking Mobile Inverted Bottleneck Convolution for EfficientNet," in *Lecture Notes in Networks and Systems*, 2023, pp. 435–445. doi: 10.1007/978-3-031-19694-2_39.

[17] V.-T. Hoang and K.-H. Jo, "Practical Analysis on Architecture of EfficientNet," in *International Conference on Human System Interaction, HSI*, 2021. doi: 10.1109/HSI52170.2021.9538782.

[18] J. P. Schwarz Schuler, S. Romani, M. Abdel-Nasser, H. Rashwan, and D. Puig, "Grouped Pointwise Convolutions Significantly Reduces Parameters in EfficientNet," in *Frontiers in Artificial Intelligence and Applications*, 2021, pp. 383–391. doi: 10.3233/FAIA210158.

[19] K. Kokufuta and T. Maruyama, "Real-time processing of contrast limited adaptive histogram equalization on FPGA," in *Proceedings - 2010 International Conference on Field Programmable Logic and Applications, FPL 2010*, 2010, pp. 155–158. doi: 10.1109/FPL.2010.37.

[20] C. Zhang, Z. Zhang, J. Liu, Y. Gao, L. Huang, and Y. Fan, "High Throughput and Low Latency Hardware of Contrast Limited Adaptive Histogram Equalization Algorithm," in *Proceedings of 2022 IEEE 16th International Conference on Solid-State and Integrated Circuit Technology, ICSICT 2022*, 2022. doi: 10.1109/ICSICT55466.2022.9963186.

[21] C. S. V, R. K, and S. Praveen P, "An Efficient Deep Learning Framework using CapsNet and SOM for Multidrug-Resistant Tuberculosis Detection and Analysis in CXR Images," *Procedia Comput. Sci.*, vol. 258, pp. 3251–3263, 2025, doi: https://doi.org/10.1016/j.procs.2025.04.583.

[22] H. Lee, H. Choo, D.-T. Le, and J. Bum, "Chest Radiographs Enhancement with Contrast Limited Adaptive Histogram," in *Proceedings of the 2023 17th International Conference on Ubiquitous Information Management and Communication, IMCOM 2023*, 2023. doi: 10.1109/IMCOM56909.2023.10035649